Demonstration of a scalable frequency-domain readout of metallic magnetic calorimeters by means of a microwave SQUID multiplexer

Sebastian Kempf (iD), Mathias Wegner, Andreas Fleischmann, Loredana Gastaldo, Felix Herrmann, Maximilian Papst, Daniel Richter, and Christian Enss

COLLECTIONS

Paper published as part of the special topic on Chemical Physics, Energy, Fluids and Plasmas, Materials Science and Mathematical Physics

View Online   Export Citation   CrossMark

ARTICLES YOU MAY BE INTERESTED IN

Simultaneous readout of 128 X-ray and gamma-ray transition-edge microcalorimeters using microwave SQUID multiplexing
Applied Physics Letters **111**, 062601 (2017); https://doi.org/10.1063/1.4986222

Demonstration of a multiplexer of dissipationless superconducting quantum interference devices
Applied Physics Letters **92**, 023514 (2008); https://doi.org/10.1063/1.2803852

Microwave SQUID multiplexer
Applied Physics Letters **85**, 2107 (2004); https://doi.org/10.1063/1.1791733

Demonstration of a scalable frequency-domain readout of metallic magnetic calorimeters by means of a microwave SQUID multiplexer

Sebastian Kempf,[a] Mathias Wegner, Andreas Fleischmann,
Loredana Gastaldo, Felix Herrmann, Maximilian Papst, Daniel Richter,
and Christian Enss
*Kirchhoff-Institute for Physics, Heidelberg University, Im Neuenheimer Feld 227,
69120 Heidelberg, Germany*

We report on the first demonstration of a scalable GHz frequency-domain readout of metallic magnetic calorimeters (MMCs) using a 64 pixel detector array that is read out by an integrated, on-chip microwave SQUID multiplexer. The detector array is optimized for detecting soft X-ray photons and the multiplexer is designed to provide a signal rise time $\tau_{\mathrm{rise}} < 400$ ns and an intrinsic energy sensitivity $\epsilon < 30\,h$. This results in an expected energy resolution $\Delta E_{\mathrm{FWHM}} < 10$ eV. We measured a signal rise time τ_{rise} as low as 90 ns and an energy resolution ΔE_{FWHM} as low as 50 eV for 5.9 keV photons. The rise time is about an order of magnitude faster compared to other multiplexed low-temperature microcalorimeters and close to the intrinsic value set by the coupling between electron and spins. The energy resolution is degraded with respect to our design value due to a rather low intrinsic quality factor of the microwave resonators that is caused by the quality of the Josephson junction of the associated rf-SQUID as well as an elevated chip temperature as compared to the heat bath. Though the achieved energy resolution is not yet compatible with state-of-the-art single-channel MMCs, this demonstration of a scalable readout approach for MMCs in combination with the full understanding of the device performance showing ways how to improve represents an important milestone for the development of future large-scale MMC detector arrays. © 2017 Author(s). All article content, except where otherwise noted, is licensed under a Creative Commons Attribution (CC BY) license (http://creativecommons.org/licenses/by/4.0/). [http://dx.doi.org/10.1063/1.4973872]

Metallic magnetic calorimeters (MMCs) are low-temperature particle detectors that use a paramagnetic temperature sensor sitting in a weak magnetic field to convert an energy input into a magnetic flux change which can be precisely measured using a superconducting quantum interference device (SQUID).[1,2] MMCs have proven to be highly suitable detectors for various applications including high-resolution X-ray spectroscopy in atomic and nuclear physics,[3,4] nuclear forensics,[5,6] radiation metrology,[7–12] direct neutrino mass determination,[13] searches for neutrinoless double beta decay[14,15] and mass spectrometry[16] since they provide an excellent energy resolution, a very fast intrinsic signal rise time, a high quantum efficiency, a large energy bandwidth as well as a highly linear detector response. State-of-the-art MMC soft X-ray detectors, for example, reach an energy resolution $\Delta E_{\mathrm{FWHM}} = 1.58$ eV for 5.9 keV photons and a signal rise time $\tau_{\mathrm{rise}} < 100$ ns. The deviation from an ideal linear detector response follows a simple quadratic energy dependence and is only 1.2% for 5.9 keV photons.[17]

Currently, individual two-stage dc-SQUIDs[18] are mostly used for reading out single channel detectors or small detector arrays. In principle, this approach could be scaled up to allow reading out large arrays. However, the linear scaling of the system complexity, the parasitic heat load as

---

[a]sebastian.kempf@kip.uni-heidelberg.de

well as cost with the number of detectors N makes this very hard or even impossible. Therefore, suitable multiplexing techniques are needed for the readout of large arrays. In the past, time-domain multiplexing (TDM) of MMCs was successfully demonstrated.[2,19] However, in TDM the white noise level of a multiplexed pixel increases with $\sqrt{N}$ due to aliasing of wideband SQUID noise[20,21] and the fast signal rise time of MMCs can't be maintained due to the small effective bandwidth per channel. In contrast, microwave SQUID multiplexing[22–24] appears to be much better suited for MMC readout since the fast signal rise time can be maintained by allocating sufficient bandwidth per channel.[25] In addition, the white noise level is independent of N. However, a demonstration of a microwave SQUID multiplexer (μMUX) based MMC readout has been lacking. Here we present the first demonstration of a μMUX based MMC readout using a 64 pixel detector array that is read out by an integrated, on-chip μMUX.

To illustrate the operation principle, we show in Fig. 1 a schematic circuit diagram of our device. Each two-pixel detector is inductively coupled to a dissipationless, non-hysteretic rf-SQUID[26,27] with loop inductance L_s and critical current I_c. For $\beta_L \equiv 2\pi L_s I_c / \Phi_0 < 1$ with $\Phi_0 = 2.067 \times 10^{-15}$ Vs denoting the magnetic flux quantum, the SQUID behaves as a non-linear inductance whose value depends on the magnetic flux Φ threading the SQUID loop. The SQUID is inductively coupled to a load inductor terminating a superconducting transmission line resonator. Due to the mutual interaction the circuit's resonance frequency is magnetic flux dependent and gets shifted as the temperature of the detector changes. For multiplexing, N resonance circuits, each employing a unique resonance frequency, are capacitively coupled to a common transmission line. Similar to microwave kinetic inductance detectors,[28,29] simultaneous readout is then achieved by injecting a microwave frequency comb and monitoring the amplitude or phase of each resonator. A modulation coil allows to apply a common magnetic flux offset to all SQUIDs.

Fig. 2 shows several photographs of our device. It consists of two independent, linear 32 pixel detector arrays, each formed by 16 two-pixel MMCs (see Fig. 2(d)) that are placed side by side. A single detector features two 170 μm $\times$ 170 μm wide and 5 μm thick particle absorbers that are made of electroplated Au.[30] Each absorber is connected via five posts to the underlying 1.35 μm thick Ag:Er$_{330\,\mathrm{ppm}}$ temperature sensor that covers the same area as the particle absorber. Underneath both
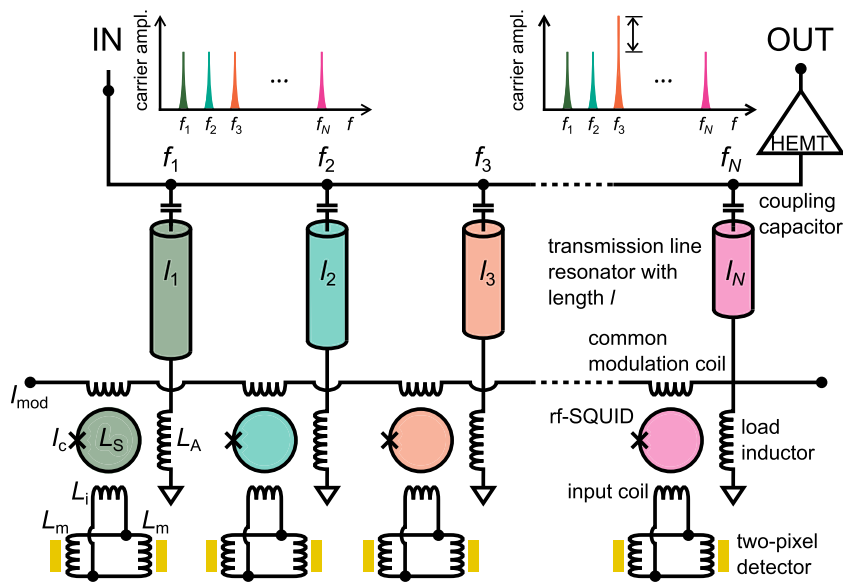

FIG. 1. Schematic circuit diagram of the 64 pixel MMC detector array that is read out by an on-chip, integrated microwave SQUID multiplexer. Each detector consists of two meander-shaped pickup coils that are equipped with a planar paramagnetic temperature sensor. Both pickup coils are connected in parallel with the input coil of the associated non-hysteretic rf-SQUID via superconducting striplines. The insets show as an example the sent and received frequency combs when performing an amplitude based μMUX readout and assuming a detector event in channel 3. More details on the actual detector and SQUID geometry can be found in Fig. 2.
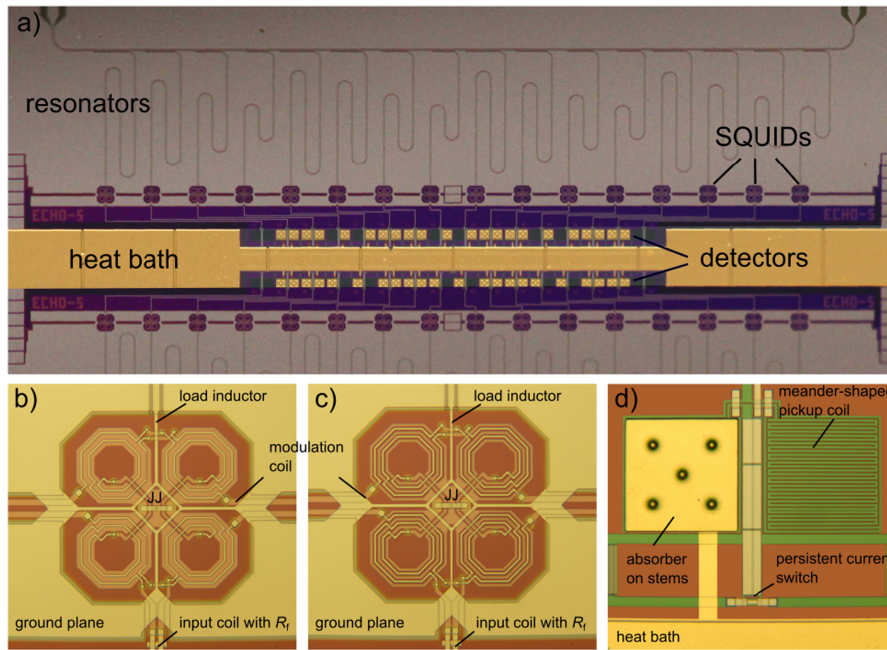
FIG. 2. Photographs of the detector array with on-chip, integrated μMUX: a) Overview of the upper two-thirds of the device. b) SQUID formed by four continuous washers connected in parallel. c) SQUID formed by four slotted washers connected in parallel. d) Two-pixel detector for which only one meander-shaped pickup coil is equipped with a temperature sensor and an absorber.

temperature sensors, a meander-shaped pickup coil with $3\,\mu$m linewidth and $6\,\mu$m pitch is placed. The inductance L_m of each pickup is $1.9\,$nH. Both pickup coils are connected in parallel with the input coil of the associated current-sensing rf-SQUID. This circuitry not only allows storage of a persistent current inside the pickup coils for creation of the required detector magnetic bias, but also enable read-out of two pixels using one SQUID channel. To prevent microwave power to leak into the detector, a resistor with $R_f = 2\,\Omega$ is placed in parallel to the input coil to form a low-pass filter (see Fig. 1). The signal decay time $\tau_{\text{decay}} \simeq 1\,$ms is adjusted by electrically connecting each sensor to an on-chip heat bath made of electroplated Au.

Each rf-SQUID is a second-order parallel gradiometer that is formed by four either continuous (see Fig. 2(b)) or slotted (see Fig. 2(c)) octagonal washers. We used both kinds of washer geometries to experimentally test the difference in the inductive and capacitive coupling between the SQUID and its input coil. We expected that the capacitive coupling between the SQUID and its input coil is much reduced for slotted washers while the magnetic coupling should be hardly affected as seen from simulations with InductEx.[31] Table I summarizes the SQUID inductance L_s, the input coil inductance L_i, as well as the mutual inductances M_{is} and M_{mod} between the SQUID, its input coil, and the modulation coil, respectively, for both kinds of washer geometries. The design critical current of the Josephson junctions is $I_c = 5\,\mu$A.

The coplanar transmission line resonators have a resonance frequency f_r between $4\,$GHz and $8\,$GHz. The design loaded quality factor is $Q_l = 5000$ and is adjusted by the coupling capacitor C_c.

TABLE I. Summary of the inductances L_s and L_i as well as the mutual inductances M_{is} and M_{mod} for a SQUID with continuous (cont.) and slotted (slot.) washer. Note that this values don't include the screening due to the superconducting flux transformer.

washer	L_s (pH)	L_i (nH)	M_{is} (pH)	M_{mod} (pH)
cont.	36.4	2.0	146.6	49.8
slot.	39.8	2.3	129.6	45.9

Depending on the resonance frequency, we therefore expect a signal rise time between 200 ns and 400 ns. The mutual inductance between the SQUID and the load inductance is $M_T \sim 7$ pH. Depending on the SQUID type and the resonance frequency f_r, the expected intrinsic energy sensitivity of the SQUIDs range from $5\,h$ and $30\,h$ when assuming an optimized readout power,[32] i.e. the current that is created inside the SQUID equals about $\Phi_0/2\pi$, and taking into account the measured overall noise temperature $T_N = 7$ K of our system. This translates into an expected energy resolution $\Delta E_{FWHM} < 10$ eV.

We mounted the device on a sample holder that was screened with superconducting material and attached it to the mixing chamber of a dilution refrigerator. Due to spatial constraints on our printed circuit board which we used for electrically connecting the device we read out only one of the two detector arrays. Before entering the device, the microwave signal was damped by 20 dB via two 10 dB attenuators mounted at the 1.5 K and 600 mK temperature stage as well as a 20 dB directional coupler mounted at the mixing chamber. The transmitted signal was passed through an isolator, a bias-tee and a cryogenic HEMT amplifier. To provide a flux bias signal and to bias the detectors, we attached a current source each to the modulation coil as well as to the detector bias lines. We used a vector network analyzer to record transmission curves $|S_{21}|^2(f)$ for different static currents I_{mod} running through the modulation coil. For the actual demonstration of a μMUX based MMC readout, we used a homodyne detection technique employing a microwave synthesizer and an I/Q mixer. We used a phase shifter to maximize the signal in the I port of the mixer and used this signal as a measure for the amplitude of the detectors, i.e. we didn't simultaneously sample both the I and the Q port of the mixer.

By measuring the transmission spectrum $|S_{21}|^2(f)$ of the multiplexer for a static magnetic flux Φ threading the SQUID loop, we were able to identify 15 resonators. One resonance was missing due to currently unknown reasons. The intrinsic quality factors Q_i of the resonators including all losses related to the SQUID, the input circuitry or the detectors itself range from 1000 to 5000 and average around $Q_i \approx 3000$. By stepwise varying the magnetic flux and acquiring transmission curves $|S_{21}|^2(f)$, we verified that all SQUIDs are operational. Fig. 3 shows, for example, several transmission curves of channel 4. The analysis of the magnetic flux dependence $f_r(\Phi)$ of the resonance frequency revealed that the geometric SQUID parameters such as the mutual inductances M_{mod} and M_T are close to our design values. Our analysis further showed that the hysteresis parameter β_L ranges between 0.4 and 0.8. Using our numerically calculated value for L_s, we determined the critical current I_c to range between 6 μA and 12 μA where the scattering is consistent with our current fabrication yield.

Fig. 3(b) shows an interesting feature of the SQUID characteristics which has not been reported so far. We observe that the intrinsic quality factor is not only rather low but also depends periodically on the magnetic flux threading the SQUID loop. This effect isn't predicted by a simple
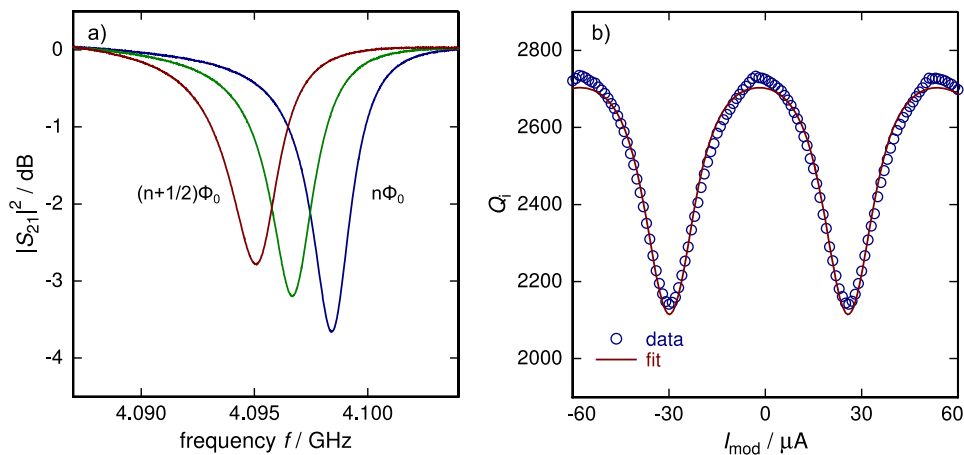

FIG. 3. (a) Transmission curve $|S_{21}|^2(f)$ of channel 4 for three different values of the magnetic flux threading the SQUID loop. (b) Magnetic flux dependence of the intrinsic quality factor of the resonator of channel 4 as well as a fit assuming a small subgap resistance of the Josephson junction.

model assuming the SQUID to be a flux-dependent inductor. However, if we include that the junction is resistively shunted by its subgap resistance, we can model the SQUID behavior very well. From this model which will be discussed in more detail elsewhere,[33] we extract a subgap resistance $R_{sg} \approx 100\,\Omega$. Though this value is about three order of magnitudes lower than our typical values,[34] it is consistent with the measured subgap resistance of unshunted junctions that were fabricated shortly after this batch and shows that we have to optimize our junction fabrication process again.

For demonstration of a μMUX based MMC readout, we prepared a persistent current I_F inside the detectors, stabilized the cryostat at $T = 20\,mK$ and acquired successively detector events for each channel. By setting an magnetic flux offset via the modulation coil, we ensured that each SQUID is biased at the steepest point of its flux-to-voltage characteristics during its measurement. Fig. 4(a) shows raw signals for three prototypical channels. The signal decay time τ_{decay} ranges between $280\,\mu$s and $350\,\mu$s and is hence a factor ~ 3 faster than our design value. The signal height $\delta\Phi$ ranges from $50\,m\Phi_0$ to $70\,m\Phi_0$ and is again about a factor ~ 3 smaller compared to the value as expected from the thermodynamical properties of the sensor material and the detector geometry. Most likely, the detector array thermally decouples from the mixing chamber. This explanation is supported by the observation that the magnetization signal of a non-gradiometric detector saturate for temperatures $T \leq 50\,mK$. By varying the readout power or strongly pumping a neighboring resonator, we proved that the microwave readout isn't causing this heating. Most likely, the coaxial cables are insufficiently heat sunk and bring parasitic heat to the device. The measured signal rise time τ_{rise} is between $80\,ns$ and $200\,ns$. The rise time is hence about an order of magnitude faster compared to other multiplexed low-temperature microcalorimeters and close to the intrinsic value set by the coupling between electron and spins. Moreover, for most channels it is consistent with the loaded quality factor Q_l of the resonator. For a few channels with very low loaded quality factor, $Q_l \simeq 1000$, τ_{rise} is slower than the resonator response time. Here, τ_{rise} nicely agrees with the intrinsic detector rise time. By this measurement we were therefore able to show that the signal rise time can be maintained when allocating sufficient bandwidth to each pixel. Depending on the actual application, we can hence find a compromise between multiplexing factor and time resolution.

To measure noise as well as to determine the energy resolution, we acquired successively several thousand detector events for channels 4, 7 and 12. Since the superconducting shield had a rather large hole to allow the X-ray photons from the external ^{55}Fe source to enter the detector array, the SQUID was influenced by environmental disturbances. Without any compensation, the flux-to-voltage transfer coefficient changed between zero and its maximum value during this measurement. We therefore implemented a slow flux feedback by adjusting the static magnetic flux offset of the SQUID according to the mean SQUID voltage for an integration time of about 1 s. Fig. 4(b) shows the noise spectra of channels 4, 7, and 12 as calculated from untriggered baselines. The measured white noise level ranges from $0.8\,\mu\Phi_0/\sqrt{Hz}$ to $1.2\,\mu\Phi_0/\sqrt{Hz}$. To compare these values to theory, we
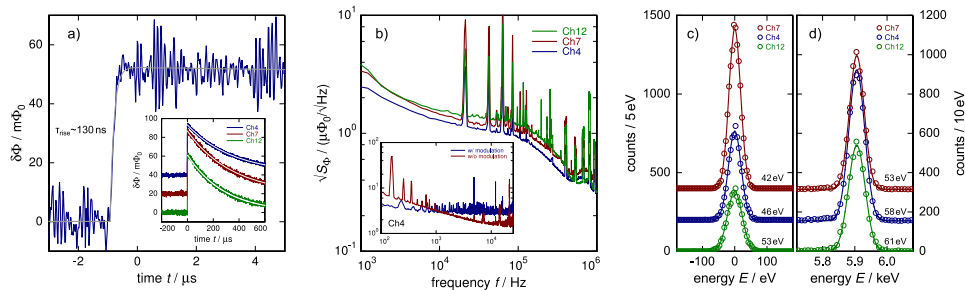

FIG. 4. (a) Signal rise of a raw signal of channel 4. The grey line is a fit assuming an exponential time dependence. The inset shows raw signals for channels 4, 7, and 12. The white solid lines show fits to the signal decay assuming a single exponential time dependence. (b) Measured noise spectra of channels 4, 7, and 12 as calculated from untriggered baselines. The low-pass characteristic at high frequencies is due to a low-pass filter. The inset shows noise spectra of channel 4 that were acquired with and without flux ramp modulation. (c) Measured baseline spectra as well as (d) Mn K_α fluorescence spectra of channels 4, 7, and 12. The solid lines show a Gaussian energy distribution with a width given in the figure.

calculate the expected white noise level for channel 4 showing $Q_l \approx 1700$ and peak-to-peak frequency shift $\Delta f_r^{max} = 3.2\,\mathrm{MHz}$. Taking into account the applied microwave power $P_{rf} \approx -(70 \pm 5)\,\mathrm{dBm}$ (the actual value depends on the currently unknown insertion loss of the different passive microwave devices at low temperatures) as well as the measured multiplexer parameters, we expect a white noise level $(0.6 \pm 0.3)\,\mu\Phi_0/\sqrt{\mathrm{Hz}}$ that agrees with our measurement. This agreement also shows how to improve the device performance. Most importantly, we need to increase the intrinsic quality factor by improving the subgap resistance of our Josephson junctions. Assuming $Q_l = 5000$ (as originally intended in our design), we expect a white noise level as low as $(0.2 \pm 0.1)\,\mu\Phi_0/\sqrt{\mathrm{Hz}}$. At low frequencies the noise spectra show a rather large low-frequency noise contribution with an amplitude $\sqrt{S_{\Phi,1/f}}(1\,\mathrm{Hz})$ ranging from $35\,\mu\Phi_0/\sqrt{\mathrm{Hz}}$ to $42\,\mu\Phi_0/\sqrt{\mathrm{Hz}}$ and a noise exponent $\alpha \approx 0.8$. Flux ramp modulation[35,36] effectively cancels this noise contribution (see inset of Fig. 4(b)). So, we attribute this noise contribution to effects in the resonators.[29,37–39]

Fig. 4(c) shows the measured energy spectra for channels 4, 7, and 12. The energy resolution ΔE_{FWHM} for $5.9\,\mathrm{keV}$ photons ranges from $50\,\mathrm{eV}$ to $60\,\mathrm{eV}$. The baseline resolution is about $10\,\mathrm{eV}$ lower. For comparison to our expectation, we again want to calculate the expected energy resolution for channel 4. Assuming a chip temperature $T = 50\,\mathrm{mK}$ (see above), we expect an energy resolution $\Delta E_{FWHM} \approx 40\,\mathrm{eV}$ which is in good agreement with our measured value. We attribute the remaining deviation as well as the additional line broadening for $5.9\,\mathrm{keV}$ photons to pronounced peaks in the noise spectrum which are related to the HEMT power supply as well as the unstable working point of the SQUID. Though providing slow flux feedback (see above), we were not able to fully stabilize the working point resulting in a time-varying SQUID gain which translates into a degraded energy resolution. However, the nice agreement between our measurements and our numerical detector model reveals that under ideal conditions, i.e. with improved loaded quality factors, heat sinking of the coaxial cables as well as superconducting shielding, an energy resolution $\Delta E_{FWHM} < 10\,\mathrm{eV}$ for a multiplexed MMC detector array is certainly within reach.

In conclusion we have demonstrated a μMUX based MMC readout which can be scaled up for reading out future detector arrays. We characterized a 64 pixel detector array that is read out by an integrated on-chip microwave SQUID multiplexer using a single channel readout scheme. We have shown that the intrinsic fast detector rise time can be maintained when allocating sufficient bandwidth to each detector channel. We measured an energy resolution ΔE_{FWHM} as low as $\leq 60\,\mathrm{eV}$ for $5.9\,\mathrm{keV}$ photons. Though the achieved energy resolution is not yet compatible with state-of-the-art single-channel MMCs, this demonstration of a scalable readout approach for MMCs represents an important milestone for the development of future large-scale MMC detector arrays. This statement is strongly supported by the full understanding of the device performance as seen from the comparison between our measurements and our numerical detector model. This comparison shows ways how to improve and more importantly that under ideal conditions an energy resolution $\Delta E_{FWHM} < 10\,\mathrm{eV}$ for a multiplexed MMC detector array is certainly within reach.

[1] A. Fleischmann, C. Enss, and G. M. Seidel, "Metallic magnetic calorimeters," in *Cryogenic Particle Detection*, edited by C. Enss (Springer, Berlin, Heidelberg, 2005).
[2] S. R. Bandler, K. D. Irwin, D. Kelly, P. N. Nagler, J.-P. Porst, H. Rotzinger, J. E. Sadleir, G. M. Seidel, S. J. Smith, and T. R. Stevenson, "Magnetically coupled microcalorimeters," J. Low Temp. Phys. **167**, 254–268 (2012).
[3] C. Pies, S. Schäfer, S. Heuser, S. Kempf, A. Pabinger, J.-P. Porst, P. Ranitzsch, N. Foerster, D. Hengstler, A. Kampkötter, T. Wolf, L. Gastaldo, A. Fleischmann, and C. Enss, "maxs: Microcalorimeter arrays for high-resolution x-ray spectroscopy at gsi/fair," J. Low Temp. Phys. **167**, 269–279 (2012).
[4] D. Hengstler, M. Keller, C. Schötz, J. Geist, M. Krantz, S. Kempf, L. Gastaldo, A. Fleischmann, T. Gassner, G. Weber, R. Märtin, T. Stöhlker, and C. Enss, "Towards fair: First measurements of metallic magnetic calorimeters for high-resolution x-ray spectroscopy at gsi," Phys. Scr. **T166**, 014054 (2015).

5 C. Bates, C. Pies, S. Kempf, L. Gastaldo, A. Fleischmann, C. Enss, and S. Friedrich, "Development of mmc gamma detectors for nuclear analysis," J. Low Temp. Phys. **176**, 631–636 (2014).

6 C. Bates, C. Pies, S. Kempf, D. Hengstler, A. Fleischmann, L. Gastaldo, C. Enss, and S. Friedrich, "Reproducibility and calibration of mmc-based high-resolution gamma detectors," Appl. Phys. Lett. **109**, 023513 (2016).

7 M. Loidl, E. Leblanc, M. Rodrigues, J. Bouchard, B. Censier, T. Branger, and D. Lacour, "Metallic magnetic calorimeters for absolute activity measurement," J. Low Temp. Phys. **151**, 1055–1060 (2008).

8 H. Rotzinger, M. Linck, A. Burck, M. Rodrigues, M. Loidl, E. Leblanc, L. Fleischmann, A. Fleischmann, and C. Enss, "Beta spectrometry with magnetic calorimeters," J. Low Temp. Phys. **151**, 1087–1093 (2008).

9 M. Loidl, M. Rodrigues, B. Censier, S. Kowalski, X. Mougeot, P. Cassette, T. Branger, and D. Lacour, "First measurement of the beta spectrum of ^{241}pu with a cryogenic detector," Appl. Rad. and Isot. **68**, 1454 (2010).

10 P. C. Ranitzsch, S. Kempf, A. Pabinger, C. Pies, J.-P. Porst, S. Schäfer, A. Fleischmann, L. Gastaldo, C. Enss, Y. S. Jang, I. H. Kim, M. S. Kim, Y. H. Kim, J. S. Lee, K. B. Lee, M. K. Lee, S. J. Lee, W. S. Yoon, and Y. N. Yuryev, "Development of cryogenic alpha spectrometers using metallic magnetic calorimeters," Nucl. Instr. Meth. A **652**, 299–301 (2011).

11 G. A. Kazakov, V. Schauer, J. Schwestka, S. P. Stellmer, J. H. Sterba, A. Fleischmann, L. Gastaldo, A. Pabinger, C. Enss, and T. Schumm, "Prospects for measuring the ^{229}th isomer energy using a metallic magnetic microcalorimeter," Nucl. Instr. Meth. A **735**, 229–239 (2014).

12 M. Loidl, C. Le-Bret, M. Rodrigues, and X. Mougeot, "Evidence for the exchange effect down to very low energy in the beta decays of ^{63}ni and ^{241}pu," J. Low Temp. Phys. **176**, 1040 (2014).

13 L. Gastaldo, K. Blaum, A. Doerr, C. Düllmann, K. Eberhardt, S. Eliseev, C. Enss, A. Faessler, A. Fleischmann, S. Kempf, M. Krivoruchenko, S. Lahiri, M. Maiti, Y. N. Novikov, P.-O. Ranitzsch, F. Simkovic, Z. Szusc, and M. Wegner, "The electron capture ^{163}ho experiment echo," J. Low Temp. Phys. **176**, 876–884 (2014).

14 M. Loidl, M. Rodrigues, X.-F. Navick, A. Fleischmann, L. Gastaldo, and C. Enss, "Concept of metallic magnetic calorimeters for rare event search in the lumineu project," J. Low Temp. Phys. **176**, 624–630 (2014).

15 D. Gray, C. Enss, A. Fleischmann, L. Gastaldo, C. Hassel, D. Hengstler, S. Kempf, M. Loidl, X. F. Navick, and M. Rodrigues, "The first tests of a large-area light detector equipped with metallic magnetic calorimeters for scintillating bolometers for the lumineu neutrinoless double beta decay search," J. Low Temp. Phys. **184**, 904–909 (2016).

16 O. Novotny, S. Allgeier, C. Enss, A. Fleischmann, L. Gamer, D. Hengstler, S. Kempf, C. Krantz, A. Pabinger, C. Pies, D. W. Savin, D. Schwalm, and A. Wolf, "Cryogenic micro-calorimeters for mass spectrometric identification of neutral molecules and molecular fragments," J. Appl. Phys. **118**, 104503 (2015).

17 A. Fleischmann *et al.*, to be submitted (2016).

18 D. Drung and M. Mück, "Squid electronics," in *The SQUID Handbook: Fundamentals and Technology of SQUIDs and SQUID Systems*, edited by J. Clarke and A. Braginski (Wiley Weinheim, 2004).

19 J.-P. Porst, S. R. Bandler, J. S. Adams, M. Balvin, J. Beyer, S. E. Busch, D. Drung, M. E. Eckart, R. L. Kelley, C. A. Kilbourne, F. S. Porter, J. E. Sadleir, G. M. Seidel, S. J. Smith, and T. R. Stevenson, "Time domain multiplexed readout of magnetically coupled calorimeters," IEEE Trans. Appl. Supercond. **23**, 2500905 (2013).

20 K. D. Irwin, L. R. Vale, N. E. Bergren, S. Deiker, E. N. Grossman, G. C. Hilton, S. W. Nam, C. D. Reintsema, D. A. Rudman, and M. E. Huber, "Time-division squid multiplexers," AIP Conference Proceedings **605**, 301–304 (2002).

21 K. D. Irwin, "Squid multiplexers for transition-edge sensors," Physica C **368**, 203–210 (2002).

22 K. D. Irwin and K. W. Lehnert, "Microwave squid multiplexer," Appl. Phys. Lett. **85**, 2107–2109 (2004).

23 K. D. Irwin, J. A. Beall, W. B. Doriese, W. D. Duncan, G. C. Hilton, J. A. B. Mates, C. D. Reintsema, D. R. Schmidt, J. N. Ullom, L. R. Vale, B. L. Zink, and K. W. Lehnert, "Microwave squid multiplexers for low-temperature detectors," Nucl. Instr. Meth. A **559**, 802–804 (2006).

24 J. A. Mates, G. C. Hilton, K. D. Irwin, L. R. Vale, and K. W. Lehnert, "Demonstration of a multiplexer of dissipationless superconducting quantum interference devices," Appl. Phys. Lett. **92**, 023514 (2008).

25 K. D. Irwin, "Shannon limits for low-temperature detector readout," AIP Conference Proceedings **1185**, 229–236 (2009).

26 P. K. Hansma, "Superconducting single-junction interferometers with small critical currents," J. Appl. Phys. **44**, 4191–4194 (1973).

27 R. Rifkin, D. A. Vincent, B. S. Deaver, and P. K. Hansma, "rf squid's in the nonhysteretic mode: Detailed comparison of theory and experiment," J. App. Phys. **47**, 2645–2650 (1976).

28 B. Mazin, "Microwave kinetic inductance detectors: The first decade," AIP Conference Proceedings **1185** (2009).

29 J. Zmuidzinas, "Superconducting microresonators: Physics and applications," Annu. Rev. Condens. Matter Phys. **3**, 169–214 (2012).

30 For testing purposes some detectors were equipped only with one absorber.

31 C. J. Fourie, O. Wetzstein, T. Ortlepp, and J. Kunert, "Three-dimensional multi-terminal superconductive integrated circuit inductance extraction," Supercond. Sci. Technol. **24**, 25015 (2011).

32 S. Kempf, L. Gastaldo, A. Fleischmann, and C. Enss, "Microwave squid multiplexer for the readout of metallic magnetic calorimeters," J. Low Temp. Phys. **175**, 850–860 (2014).

33 M. Wegner *et al.*, to be submitted (2016).

34 S. Kempf, A. Ferring, A. Fleischmann, L. Gastaldo, and C. Enss, "Characterization of the reliability and uniformity of an anodization-free fabrication process for high-quality nb/al-alo$_x$/nb josephson junctions," Supercond. Sci. Technol. **26**, 065012 (2013).

35 K. W. Lehnert, K. D. Irwin, M. A. Castellanos-Beltran, J. A. B. Mates, and L. R. Vales, "Evaluation of a microwave squid multiplexer prototype," IEEE Trans. Appl. Supercond. **17**, 705–709 (2007).

36 J. Mates, K. Irwin, L. Vale, G. Hilton, J. Gao, and K. Lehnert, "Flux-ramp modulation for squid multiplexing," J. Low Temp. Phys. **167**, 707–712 (2012).

37 J. Gao, J. Zmuidzinas, B. A. Mazin, H. G. LeDuc, and P. K. Day, "Noise properties of superconducting coplanar waveguide microwave resonators," Appl. Phys. Lett. **90**, 102507 (2007).

[38] R. Barends, H. L. Hortensius, T. Zijlstra, J. J. A. Baselmans, S. J. C. Yates, J. R. Gao, and T. M. Klapwijk, "Contribution of dielectrics to frequency and noise of nbtin superconducting resonators," Appl. Phys. Lett. **92**, 223502 (2008).

[39] J. Gao, M. Daal, A. Vayonakis, S. Kumar, J. Zmuidzinas, B. Sadoulet, B. A. Mazin, P. K. Day, and H. G. Leduc, "Experimental evidence for a surface distribution of two-level systems in superconducting lithographed microwave resonators," Appl. Phys. Lett. **92**, 2505 (2008).